Title.

Treatment-shortening effect of a novel regimen combining high-dose rifapentine and clofazimine in pathologically distinct mouse models of tuberculosis

Running title.

Rifapentine-clofazimine in TB mouse models

Authors and affiliations.

Vikram Saini,[a,b*] Nicole C. Ammerman,[a*] Yong Seok Chang,[a] Rokeya Tasneen,[a] Richard E. Chaisson,[a] Sanjay Jain,[a#] Eric Nuermberger,[a#] Jacques H. Grosset[a]

[a]Center for Tuberculosis Research, Johns Hopkins University School of Medicine, Baltimore, Maryland, USA

[b]Current address: MedStar Health Internal Medicine, Baltimore, Maryland, USA

*These authors contributed equally to this work.

[#]Corresponding authors: Sanjay Jain, sjain5@jhmi.edu; and Eric Nuermberger, enuermb@jhmi.edu

ABSTRACT

High-dose rifapentine and clofazimine have each separately been associated with treatment-shortening activity when incorporated into tuberculosis (TB) treatment regimens. We hypothesized that both modifications, *i.e.,* the addition of clofazimine and the replacement of rifampin with high-dose rifapentine, in the first-line regimen for drug-susceptible TB would significantly shorten the duration of treatment necessary for cure. We tested this hypothesis in a well-established BALB/c mouse model of TB chemotherapy and also in a C3HeB/FeJ mouse model in which mice can develop caseous necrotic lesions, an environment where rifapentine and clofazimine may individually be less effective. In both mouse models, replacing rifampin with high-dose rifapentine and adding clofazimine in the first-line regimen resulted in greater bactericidal and sterilizing activity than either modification alone, suggesting that a rifapentine- and clofazimine-containing regimen may have the potential to significantly shorten the treatment duration for drug-susceptible TB. These data provide preclinical evidence supporting the evaluation of regimens combining high-dose rifapentine and clofazimine in clinical trials.

INTRODUCTION

In its most recent global tuberculosis (TB) report, the World Health Organization (WHO) estimated that 10 million incident cases of TB occurred in 2017, highlighting that the global TB epidemic is tragically far from controlled (1). This sustained burden of TB occurs despite the existence of a highly efficacious regimen for treatment of drug-susceptible TB, which accounted for about 9.4 million or 94% of the estimated TB cases in 2017. Many factors, ranging from individual to programmatic levels, and varying widely in nature and by environment, contribute to barriers that prevent patients with TB from receiving or completing curative treatment (2); one such factor that globally impacts TB control is the duration of treatment.

The first-line regimen for treatment of drug-susceptible TB consists of daily administration of four drugs (rifampin, isoniazid, pyrazinamide, and ethambutol) for at least two months, followed by an additional four months of daily rifampin and isoniazid (3, 4). In addition to the burden on individual patients, administration of a six-month, multidrug regimen requires significant resources from a public health perspective, especially if treatment is directly observed as is recommended (5, 6). Incomplete administration can lead to treatment failure and the selection and spread of drug-resistant *Mycobacterium tuberculosis*; thus, curative regimens of shorter duration could significantly improve global TB control efforts.

In a well-established BALB/c mouse model of TB chemotherapy (7), increasing the rifamycin exposure, especially by replacing rifampin with daily high-dose rifapentine,

significantly decreased the duration of treatment necessary to achieve relapse-free cure (8, 9). These relapse-based preclinical studies were among critical data supporting the evaluation of high-dose rifapentine in a phase 2 clinical trial for treatment of drug-susceptible TB (ClinicalTrials.gov identifier NCT00694629), where higher rifapentine exposures were strongly associated with higher bactericidal activity. A phase 3 trial is currently underway to determine whether replacing rifampin with high-dose rifapentine can shorten the treatment of drug-susceptible TB to four months (ClinicalTrials.gov identifier NCT02410772).

The anti-leprosy drug clofazimine has been indirectly associated with treatment-shortening when incorporated into regimens for multidrug-resistant- (MDR-) TB (10-15). In a BALB/c mouse model of MDR-TB chemotherapy, clofazimine specifically and directly contributed potent bactericidal and treatment-shortening activity to a regimen of second-line drugs (16), and in 2016, the WHO included clofazimine in its “Shorter MDR-TB Regimen,” referring specifically to the sterilizing (*i.e.*, treatment-shortening) activity that this drug may add to the regimen (17). The addition of clofazimine to the first-line regimen was also evaluated in BALB/c mice, where again it was shown to directly contribute significant activity, shortening the duration of treatment necessary to achieve relapse-free cure by up to 2 months (18, 19). The addition of clofazimine to the first-line regimen is currently being evaluated in the phase 2/3 TRUNCATE-TB study (ClinicalTrials.gov identifier NCT03474198).

Because replacement of rifampin with high-dose rifapentine in the first-line regimen and the addition of clofazimine separately added substantial treatment-shortening activity in the BALB/c mouse model, we hypothesized that combining these modifications would contribute greater treatment-shortening activity than either modification alone. To test this hypothesis, we used the BALB/c mouse model to directly compare the bactericidal and sterilizing activity of four daily regimens: (i) the first-line regimen; and the same regimen with either (ii) addition of clofazimine; (iii) replacement of rifampin with high-dose rifapentine; or (iv) the same regimen with both addition of clofazimine and replacement of rifampin with high-dose rifapentine.

The BALB/c mouse model is commonly used for preclinical studies to evaluate the efficacy of novel drug regimens (7). However, whereas human TB disease is associated with both intracellular bacteria and a large extracellular bacterial population in necrotic caseous lesions and cavities (20), the BALB/c model creates only cellular lung lesions with intracellular (mostly intra-macrophage) bacilli and specifically lacks the caseous hallmarks of human TB, raising concerns that it may not fully represent the activity of drugs and regimens across the full spectrum of human disease (7, 21-24). Both rifapentine and clofazimine are known to accumulate within macrophages (25, 26), and it has also been reported that both of these drugs do not diffuse well into caseous lesions (27-30). Therefore, it is possible that the BALB/c mouse model could overestimate the activity of these two particular drugs. To address this issue, we also evaluated the same four regimens in a C3HeB/FeJ mouse model of TB. In this model, mice can develop necrotic caseous lung lesions with a significant extracellular bacterial

103 population and even lung cavities (7, 22-24, 31-35). The standard TB treatment regimen
104 performs similarly in this model as in the BALB/c model (9, 22, 36-38), thus allowing for
105 the specific evaluation of clofazimine and rifapentine activity in this disease setting.
106
107 **RESULTS**
108 The scheme of the study is presented in **Table 1**. The primary outcome of this study
109 was the proportion of mice with relapse-free cure, *i.e.,* culture-negative lungs six months
110 after stopping treatment. The secondary endpoint was bactericidal activity, *i.e.*, the
111 decline of *M. tuberculosis* colony-forming unit (CFU) counts during treatment.
112
113 **Establishment of infection: BALB/c mice**
114 The day after aerosol infection with *M. tuberculosis* strain H37Rv, the mean bacterial
115 implantation was 4.25 (SD 0.15) $\log_{10}$ CFU/lung (**Figs. 1**, **S1**; **Tables S1**, **S2**). Two
116 weeks later, at treatment initiation, the mean bacterial burden in the lungs increased to
117 7.13 (SD 0.11) $\log_{10}$ CFU/lung (**Table S3**). As expected in this model (7), the untreated
118 negative control mice became moribund three weeks after infection and were
119 euthanized; these mice had a mean bacterial burden of 8.39 (SD 0.16) $\log_{10}$ CFU/lung
120 (**Table S3**), and evenly distributed, small, uniform lung lesions were observed (**Fig. S2**).
121
122 **Assessment of bactericidal activity: BALB/c mice**
123 The RHZE control regimen performed as expected in this model, resulting in killing of
124 2.3 $\log_{10}$ CFU/lung by 4 weeks, with additional killing thereafter of approximately 1 $\log_{10}$
125 CFU per two weeks (**Fig. 1**; **Tables S4-S8**). After 12 weeks of treatment, all RHZE-

126 treated mice remained culture positive with a mean bacterial burden of 0.70 (0.22) $\log_{10}$
127 CFU/lung, and lung lesions were still visible (**Figs. S3-S7**). Compared to RHZE, the
128 clofazimine-containing RHZEC regimen significantly increased the bactericidal activity
129 by 0.8-1.0 $\log_{10}$ CFU/lung at each time point ($p < 0.0001$ at each time point), and all
130 mice were culture-negative by 12 weeks. Replacement of rifampin with high-dose
131 rifapentine had an even larger effect on the activity of the standard regimen.
132 Administration of PHZE increased the bactericidal activity by 1.3 $\log_{10}$ CFU/lung at 4
133 weeks and by about 2.5 $\log_{10}$ CFU/lung at both 6 and 8 weeks compared to
134 administration of RHZE ($p < 0.0001$ at each time point). Except for one mouse with a
135 single CFU, the mice receiving PHZE were culture-negative by 10 weeks, and this
136 regimen was also associated with significantly lower lung CFU counts than the RHZEC
137 regimen ($p < 0.01$ at all time points up to 10 weeks). Despite that the lungs of PHZE-
138 treated mice had significantly lower CFUs than the lungs of RHZEC-treated mice, gross
139 lung lesions were consistently more visible in the PHZE-treated mice (**Figs. S3-S7**).
140 Finally, replacement of rifampin with high-dose rifapentine plus clofazimine had the
141 most potent bactericidal activity of all regimens tested. PHZEC was significantly more
142 bactericidal than the PHZE regimen and all time points up to 8 weeks ($p < 0.0001$ at
143 each time point), when mice receiving PHZEC became culture-negative.
144
145 **Assessment of sterilizing activity: BALB/c mice**
146 The raw lung CFU data at relapse assessment in mice treated for 6, 8, 10, and 12
147 weeks are presented in **Tables S9**, **S10**, **S11**, and **S12**, respectively. As expected,
148 nearly all mice (19/20) that received RHZE for 12 weeks were culture-positive 6 months

after stopping treatment (**Table 2**; **Fig. S8**). Among mice treated with RHZEC for 10 weeks, nearly one-half experienced relapse, but no relapses occurred in mice that received this regimen for 12 weeks ($p < 0.0001$). Thirty percent of mice that received PHZE for 8 weeks relapsed, and relapse occurred in only one mouse that received this regimen for 10 weeks. Similarly, thirty percent relapse was observed in mice that received PHZEC for 6 weeks, and no relapses occurred in mice that received this regimen for 8 weeks ($p = 0.09$). However, there were two relapses among the mice that received PHZEC for 10 weeks, with one mouse yielding only a single CFU at relapse assessment (**Table S11**). Finally, there was no relapse after treatment for 12 weeks. Overall, the rank order of the regimens' bactericidal activity corresponded to their sterilizing activity, *i.e.*, PHZEC > PHZE > RHZEC > RHZE. Among culture-positive mice, the bacterial burden at relapse assessment was lowest for mice that received PHZEC (all less than 4.5 $\log_{10}$ CFU/lung for all mice regardless of treatment duration), and no mouse from any treatment group relapsed with a burden greater than 5.3 $\log_{10}$ CFU/lung (**Fig. S8**).

Establishment of infection: C3HeB/FeJ mice

The day after aerosol infection, the mean bacterial implantation was 2.03 (SD 0.13) $\log_{10}$ CFU/lung (median 2.06 $\log_{10}$ CFU/lung) (**Figs. 2A**, **S9**; **Tables S1**, **S2**). To monitor the infection status during the 6 weeks between infection and the start of treatment, we also determined the lung CFU counts 3 weeks after infection (**Table 1**). *M. tuberculosis* had multiplied to a mean burden of 6.39 (SD 0.25) $\log_{10}$ CFU/lung (median 6.45 $\log_{10}$ CFU/lung) (**Table S13**), and unevenly distributed, non-uniform, large lung lesions were

172 just visible (**Fig. S10**). During the subsequent 3 weeks, twenty-two mice died or became
173 moribund and were euthanized prior to treatment initiation. The lungs of these mice
174 were extensively diseased with large, diffuse lesions affecting entire lung lobes (**Fig.**
175 **S11**), and the mean bacterial burden in these mice was 9.14 (SD 0.21) $\log_{10}$ CFU/lung
176 (median 9.11 $\log_{10}$ CFU/lung) (**Table S14**). The mice pre-assigned for sacrifice at the
177 Day 0 time point had a mean bacterial burden of 7.46 (SD 0.75) $\log_{10}$ CFU/lung (median
178 7.20, range 6.63-8.78 $\log_{10}$ CFU/lung) (**Table S13**), and varying gross lung pathology
179 was also observed (**Fig. S12**). Lung lesions were variable in size and number and non-
180 uniformly distributed. Including the mice that died before the start of treatment, the pre-
181 treatment bacterial burden in the C3HeB/FeJ mice spanned nearly 3 $\log_{10}$, ranging from
182 6.63 to 9.59 $\log_{10}$ CFU/lung (**Fig. 2A**). Among the pre-assigned untreated negative
183 control mice, two died prior to Day 0, and the remaining mice survived 13 to 26 weeks
184 post-infection, with bacterial burdens ranging from 7.74 to 9.29 $\log_{10}$ CFU/lung at the
185 time of death (**Table S14**); the lungs of these mice were also extensively diseased (**Fig.**
186 **S13**). Overall, the course of *M. tuberculosis* infection in this C3HeB/FeJ mouse model
187 was as expected based on previous studies (24, 34, 37, 39).
188
189 **Assessment of bactericidal activity: C3HeB/FeJ mice**
190 The RHZE control regimen performed as expected in this model, resulting in killing of
191 3.5 $\log_{10}$ CFU/lung by 4 weeks (**Fig. 2B**; **Table S15**), with continued bactericidal activity,
192 albeit with more variable CFU counts, over 12 weeks (**Fig. 2C-F**), resulting in a final
193 mean bacterial burden of 0.42 (SD 0.78) $\log_{10}$ CFU/lung (only 2/5 mice were culture-
194 positive at the end of treatment). Gross lung lesions were observed in the RHZE-treated

mice up to Week 12 (**Figs. S14-S18**). After four of treatment, there was no statistically significant difference between the bactericidal activity of RHZE and any of the other three regimens (**Fig. 2B**). As with RHZE, the RHZEC, PHZE, and PHZEC regimens were all associated with bactericidal activity over 12 weeks, but at no point during treatment were statistically significant differences observed in the bacterial burdens of mice receiving these three regimens. Despite the observed variability in bacterial burden, all mice that received PHZEC became culture-negative at Week 6 (**Fig. 2C**; **Table S16**), and all mice that received PHZE became culture-negative at Week 8 (**Fig. 2D**; **Table S17**); mice receiving either of these regimens remained culture-negative at Weeks 10 and 12 (**Fig. 2D-F**; **Tables S18**, **S19**). Mice that received RHZEC became culture-negative at Week 12 (**Fig. 2E**; **Table S19**). Regimen-associated differences in gross lung pathology became visible after 6 weeks of treatment. As was observed with BALB/c mice, administration of either of the clofazimine-containing regimens was associated with a reduction in visible lesions (**Figs. S14-S18**).

Assessment of sterilizing activity: C3HeB/FeJ mice

The raw lung CFU data at relapse assessment in mice treated for 6, 8, 10, and 12 weeks are presented in **Tables S20**, **S21**, **S22**, and **S23**, respectively. As expected, approximately half of the mice (11/19) that received RHZE for 12 weeks were culture-positive 6 months after stopping treatment (**Table 2**; **Fig. S8**). Less than 50% of mice treated with RHZEC, PHZE, or PHZEC experienced culture-positive relapse after treatment durations of 10, 8, and 6 weeks, respectively. The relapse proportion for mice that received RHZE for 12 weeks was significantly higher than the relapse proportion for

mice that received ≥8 weeks of PHZEC and ≥10 weeks of treatment with PHZE ($p < 0.05$). In mice that received PHZEC for 8 and 10 weeks, there was a single relapse, and no relapse occurred at all in mice that received PHZEC for 12 weeks. As was observed with BALB/c mice, the overall rank order of the regimens' bactericidal activity in C3HeB/FeJ corresponded to their sterilizing activity, *i.e.*, PHZEC > PHZE > RHZEC > RHZE. However, the bacterial burden in the lungs of the culture-positive mice was generally much higher and more variable for the C3HeB/FeJ mice compared to the BALB/c mice (**Fig. S8**). The bacterial burden in the culture-positive C3HeB/FeJ mice ranged from a single CFU to >9 $\log_{10}$ CFU/lung.

Trough serum concentrations of clofazimine and rifapentine

At the sacrifice time points after 4, 8, and 12 weeks of treatment, the trough (about 72 hours post-dose) serum concentrations of clofazimine and rifapentine were measured in mice receiving clofazimine- and rifapentine-containing regimens, respectively (**Fig. 3**; **Table S24**). For clofazimine, the trough serum concentrations were around 1.5 μg/mL in mice receiving either RHZEC (**Fig. 3A**) or PHZEC (**Fig. 3B**), with no statistically significant differences in mean concentrations across time points or between BALB/c and C3HeB/FeJ mice. For rifapentine, differences in trough serum concentrations were observed between mouse strains and between regimens (**Figs. 3C-D**, **S19**). Rifapentine concentrations were consistently higher in the serum of BALB/c mice compared to C3HeB/FeJ mice. In mice that received PHZE, the mean serum concentration in BALB/c mice was around 8-9 μg/mL at each time point, while the mean serum concentration in C3HeB/FeJ mice was around 4-5 μg/mL (**Figs. 3C**); the differences

were statistically significant at Week 4 ($p < 0.01$) and Week 12 ($p < 0.05$). In mice that received PHZEC (**Fig. 3D**), mean rifapentine concentrations were higher in BALB/c mice (10.9 µg/mL and 12.1 µg/mL at Weeks 8 and 12, respectively) compared to C3HeB/FeJ mice (7.0 µg/mL and 10.2 µg/mL at Weeks 8 and 12, respectively), though these differences were not statistically significant. In both mouse strains, the mean rifapentine concentrations were higher in mice receiving PHZEC compared those that received PHZE. In C3HeB/FeJ mice that received PHZEC, the mean trough rifapentine concentrations were 30-50% higher than in the C3HeB/FeJ mice that received PHZE; this difference was statistically significant at Week 12 ($p < 0.01$). In BALB/c mice, mean rifapentine concentrations were 25% higher in mice that received PHZEC compared to PHZE, but the difference was not statistically significant.

DISCUSSION

The main finding of this study is that replacement of rifampin with high-dose rifapentine together with the addition of clofazimine increased the bactericidal and sterilizing activity of the first-line regimen to a significantly greater extent than either modification alone in two pathologically distinct mouse models of TB chemotherapy. While each of these modifications is currently being studied individually in TB patients, our results indicate that superior treatment-shortening effects would be observed if they were combined in the same regimen.

The independent effects of incorporating high-dose rifapentine and clofazimine into the first-line regimen in BALB/c mice were consistent with those observed in previous

studies with this model (9, 19). Aggregating the results of relapse assessments from six prior experiments that examined the impact of rifapentine or clofazimine in this model (9, 18, 19, 40) reveals that relapse was observed in 100% (30/30), 40% (23/58), 13% (4/30), and 8% (2/24) of mice treated with RHZ ±E for 12, 16, 20, and 24 weeks, respectively (**Table S25**). The consistency of these results across studies allows estimation of the effect of each modification on the duration of treatment necessary to prevent relapse. In the current study, replacement of rifampin with high-dose rifapentine reduced the percentages of mice relapsing to 30% (6/20) and 6% (1/18) after 8 and 12 weeks of treatment, respectively, indicating that this intervention reduced the treatment needed to prevent a similar number of relapses by at least 8 weeks compared to RHZE. Likewise, the addition of clofazimine reduced the percentages of mice relapsing to 56% (10/18) and 0% (0/20) after 10 and 12 weeks of treatment, respectively, indicating, as prior studies have, that the treatment duration required to prevent the majority of mice from relapsing is 4-6 weeks shorter when clofazimine is added to the first-line regimen at the 12.5 mg/kg dose. Together, these modifications appear to have an additive effect on the anti-TB activity of the first-line regimen. Combining high-dose rifapentine with clofazimine reduced the percentage of mice relapsing to 28% after 6 weeks of treatment, indicating that the combined modifications shortened the treatment needed to obtain similar number of relapses by at least 10 weeks.

Overall, the results in C3HeB/FeJ mice were quite comparable to those observed in BALB/c mice. Significant mouse-to-mouse variability in lung bacterial burden was observed which was due, in large part, to differences in disease progression prior to

287 treatment, as the pretreatment lung bacterial burden ranged from 6.63 to 9.59 $\log_{10}$
288 CFU/lung (**Fig. 2A**). The magnitude of the variability in bacterial burden within
289 C3HeB/FeJ treatment groups spanned 4 $\log_{10}$ CFU/lung in three of the four treatment
290 groups at least once during the first 6 weeks of treatment (**Fig. 2B,C**), a slightly greater
291 range than what was observed at the start of treatment, consistent with our
292 observations that the lung disease may contribute to progress in the most severely
293 affected mice after initiation of combination chemotherapy. Although there was
294 variability in trough serum concentrations of rifapentine and clofazimine in the
295 C3HeB/FeJ mice (**Fig. 3**), drug levels did not correlate with lung CFU counts at the
296 individual mouse level (**Fig. S19**, **Tables S15, S17, S24**), and serum rifapentine and
297 clofazimine concentrations were also highly variable in BALB/c mice in which there was
298 much less variability in lung CFU counts (**Figs. 1, 3, S19**). Therefore, in mice that
299 received clofazimine and/or rifapentine, the serum levels of these drugs did not appear
300 to contribute to variability in lung CFU counts during treatment. However, it is possible
301 that tissue-level, and especially lesion-specific, PK differences in C3HeB/FeJ mice
302 contribute to the observed variability in the bactericidal activity associated with each
303 regimen, a concept that has been intimated by numerous studies.
304
305 Irwin and colleagues reported that clofazimine monotherapy, administered at 20 mg/kg,
306 had limited bactericidal activity in the lungs of *M. tuberculosis*-infected C3HeB/FeJ mice
307 when treatment was initiated 6 weeks after infection; however, if treatment was initiated
308 3 weeks after infection, clofazimine had quite potent bactericidal activity (30). The
309 authors linked the diminished activity of clofazimine with the development of hypoxic,

caseous necrotic lesions containing extracellular bacteria, suggesting that clofazimine was less active within these lesions. This hypothesis was further supported by studies demonstrating that clofazimine diffuses relatively poorly into caseous necrotic lesions in humans TB (27), does not have bactericidal activity in *ex vivo* caseum from *M. tuberculosis*-infected rabbits (41), and the long-standing observation that clofazimine accumulates in macrophages (26, 27, 42, 43). Rifapentine has been shown to diffuse into necrotic caseous lesions less rapidly than rifampin in a rabbit model of cavitary TB (28), a finding that correlates with clinical data indicating that replacing rifampin with rifapentine added proportionally less activity in patients with cavitary versus non-cavitary TB disease (44). It has also been reported that rifapentine accumulates in macrophages and is relatively more active against intracellular than extracellular *M. tuberculosis* (25). Finally, we previously observed an association between large gross lung lesions in *M. tuberculosis*-infected C3HeB/FeJ mice and reduced rifapentine activity; the bactericidal activity of rifapentine at 10 mg/kg was similar to that of rifampin at 10 mg/kg in mice with the largest gross lesions and highest CFU counts (24). As such gross lung pathology in C3HeB/FeJ mice is associated with the presence of necrotic, caseating granulomatous histopathology (24, 34, 35), these data supported the hypothesis that rifapentine may be less active and/or available in the necrotic, caseating lesions. Therefore, it is possible that the apparent diminished activity of clofazimine and/or rifapentine in the large caseous lesions of some C3HeB/FeJ mice could contribute to the variability in lung CFU counts observed at Week 4, especially among mice receiving rifapentine- or clofazimine-containing regimens. (**Fig. 2B**), although our data cannot specifically address this issue.

Ultimately, and similar to what was observed in BALB/c mice, both of these drugs did individually add significant bactericidal and sterilizing activity to the first-line regimen in C3HeB/FeJ mice. Possible reasons for this include: the activity of clofazimine and rifapentine was enhanced with co-administration of isoniazid, pyrazinamide, and ethambutol; the anti-TB activity of the other drugs in the regimen allowed the lesions to begin to heal, modifying the necrotic microenvironments and making them more favorable for clofazimine and rifapentine activity; and/or that these drugs reached therapeutic levels at the site of action independent of lung pathology. Interestingly, this overall equivalent activity of the rifapentine-containing regimens was observed between mice strains despite that the trough rifapentine serum levels tended to be lower in the C3HeB/FeJ mice compared to in BALB/c mice (**Fig. 3C,D**). As the differences were only statistically significant in mice receiving PHZE at the Week 4 and Week 12 time points, it is difficult to interpret the significance, if any, of this difference. Dosing in the C3HeB/FeJ mice was adjusted to account for their increasing body mass over the course of treatment (see Methods and **Table S26**) to ensure that the mice were not under-dosed as they increased in size. Previously, PK differences were not observed in BALB/c and C3HeB/FeJ mice following a single dose of rifapentine alone at 10 mg/kg (9). Thus, further studies are needed to understand any possible long-term PK differences associated with rifapentine between these two strains of mice. Another interesting finding was that in both strains of mice, trough rifapentine levels were higher in mice that received PHZEC compared to PHZE (**Fig. 3C,D**), suggesting that the presence of clofazimine (which had trough serum levels unaffected by either regimen or

mouse strain) may somehow boost rifamycin exposures in the mice, which could in part explain why clofazimine has been shown to contribute significantly more bactericidal activity when added to RHZE than when administered as monotherapy (18, 19, 30, 45-47). Mechanisms of activity aside, this study highlights the essentiality of evaluating the long-term activity of drugs in combination in order to understand the impact of the regimen, as opposed to shorter-term studies and/or studies of single drugs, on treatment outcome.

C3HeB/FeJ mice are more susceptible to *M. tuberculosis* infection than BALB/c mice (22, 24, 33, 34), which was evidenced in this study by the number of mice that became moribund prior to the start of treatment (**Table S14**). This is a limitation of this study in that the C3HeB/FeJ mice with the most severe lung pathology were censored from regimen evaluation. This represents a common quandary with this model. A six-week incubation following aerosol infection is generally necessary to allow for the development of caseous, necrotic lesions in most C3HeB/FeJ mice (22, 24, 33-35). The risk of starting treatment earlier to capture the relatively small proportion of that rapidly succumb to disease is that the majority of the other mice will not develop the pathology that is the hallmark of and rationale for use of this model. In addition to decreasing the bacterial implantation (34), further refinements of this model are needed to limit the heterogeneity in the progression of disease following aerosol infection.

Another limitation of this study is that lung histopathology was not evaluated. We and others have presented histopathological results from this model previously and

379 demonstrated the association between size and extent of caseating lesions and
380 bacterial burden (22, 24, 32, 35). For this study, our primary and secondary endpoints of
381 culture-positive relapse (sterilizing activity) and decline in lung bacterial burden during
382 treatment (bactericidal activity), respectively, relied entirely on the detection of *M.*
383 *tuberculosis* in the mouse lungs. Therefore, it was most important to homogenize the
384 entire lung for CFU assessment. For C3HeB/FeJ mice, this was particularly important
385 due to the non-uniform and asymmetric development of lung disease in these mice
386 (**Figs. S10-S18**), which confounds estimation of total lung burden if calculated from only
387 a portion of the lung. Accordingly, we could not specifically evaluate the presence and
388 distribution of caseous, necrotic lesions in the lungs at the start of treatment. Since
389 disease in humans is heterogeneous and different pathological states can occur
390 simultaneously in the same host, getting sufficient drug to these different lesions and
391 understanding their activity within such lesions is essential for optimal anti-bacterial
392 activity (23, 32, 48). Therefore, studies in animal models replicating these different
393 pathologies is of interest during preclinical evaluations.
394
395 In conclusion, in both BALB/c and C3HeB/FeJ mouse models of TB, replacing rifampin
396 with high-dose rifapentine and adding clofazimine in the first-line regimen resulted in
397 greater bactericidal and sterilizing activity than either modification alone, suggesting that
398 a PHZEC-based regimen may have the potential to significantly shorten the treatment
399 duration for drug-susceptible TB. High-dose rifapentine and clofazimine are each
400 currently being evaluated separately in clinical trials as part of a first-line regimen for TB
401 treatment (ClinicalTrials.gov identifiers NCT02410772 and NCT03474198). The

preclinical data presented here provide evidence supporting the clinical evaluation of a regimen combining high-dose rifapentine with clofazimine for treatment of drug-susceptible TB.

MATERIALS AND METHODS

Study design

The final scheme of the study is presented in **Table 1**. The original study protocol included 315 and 328 BALB/c and C3HeB/FeJ mice, respectively. To mitigate losses of C3HeB/FeJ mice, which are more susceptible to *M. tuberculosis* than BALB/c mice (22, 24, 33, 34), we infected an additional 25 mice, for a total of 353 C3HeB/FeJ mice. The primary outcome of this study was the proportion of mice with relapse-free cure, *i.e.,* culture-negative lungs six months after stopping treatment. The secondary endpoint was bactericidal activity, *i.e.*, the decline of *M. tuberculosis* CFU counts during treatment.

Animals

Female BALB/c mice, aged 5 weeks, were obtained from Charles River Laboratories. Female C3HeB/FeJ mice, aged 4-6 weeks, were obtained from The Jackson Laboratory. All mice were housed in a biosafety level 3 vivarium in individually ventilated cages with sterile wood shavings for bedding. Up to five mice were housed per cage with access to food and water *ad libitum*. Room temperature was maintained at 22-24°C with a 12-hour light/dark cycle. All mice were sacrificed by intentional isoflurane overdose (drop method) followed by cervical dislocation.

425

426 **Aerosol infections**

427 *M. tuberculosis* strain H37Rv (American Type Culture Collection strain ATCC 27294)
428 was used for aerosol infections. This stock is susceptible to all drugs used in this study.
429 Bacterial stocks were cultured as previously described (45). To achieve a relatively
430 high-burden infection in BALB/c mice, an actively growing bacterial culture with an
431 optical density at 600 nm (OD_{600}) of 1.04 was used directly for aerosol infection. To
432 achieve a low-burden infection in C3HeB/FeJ mice, frozen stock (prepared from a
433 culture with an OD_{600} of 1.04) was thawed and diluted 15-fold in phosphate-buffered
434 saline for aerosol infection. The concentration of each bacterial suspension used for
435 infection was determined as previously described (45) and as detailed in **Table S1**.
436 Mice were infected by aerosol using a full-size Glas-Col Inhalation Exposure System
437 according to the manufacturer's instructions. BALB/c and C3HeB/FeJ mice were
438 infected in three and four infection runs, respectively. To determine the number of
439 bacteria delivered to the lungs, three mice from each infection run were sacrificed the
440 day after infection, and lung CFU counts were determined as previously described (45)
441 and as detailed in **Table S2**.

442

443 **Treatment**

444 BALB/c mice were randomized (stratified by infection run) and assigned to treatment
445 groups and sacrifice cohorts two days before the start of treatment. C3HeB/FeJ mice
446 were randomized (stratified by infection run) nine days before the start of treatment;
447 subsequently, we observed the development of significant variation in body mass of the

mice. Therefore, two days before the start of treatment, C3HeB/FeJ mice were randomized again, this time stratified only by body mass (groups of <24, 24 to 25, 25 to <26.5, 26.5 to 28, and >28 g), and then assigned to treatment groups and sacrifice cohorts. Untreated negative control mice were not randomized but followed separately to monitor infection outcome by aerosol infection run. Treatment was initiated on Day 0, which was two and six weeks after infection for BALB/c and C3HeB/FeJ mice, respectively. Three mice from each infection run were sacrificed on Day 0 to determine the lung CFU counts. All pretreatment lung CFU counts were determined as previously described (45).

The regimens evaluated in this study are presented in **Table 1**. Untreated mice served as the negative control group to verify the virulence of the *M. tuberculosis* infection. The first-line regimen, daily rifampin (R, 10 mg/kg), isoniazid (H, 10 mg/kg), pyrazinamide (Z, 150 mg/kg), and ethambutol (E, 100 mg/kg), was administered as a positive control; these doses for mice are well-established for approximating the area under the plasma concentration-time curve (AUC) produced by recommended doses in humans (49, 50). Three modifications of the standard regimen were evaluated. In regimen RHZEC, clofazimine (C, 12.5 mg/kg) was added to the first-line regimen; although the human pharmacokinetic profile of clofazimine is not well understood, this dose appears to result in steady-state blood concentrations similar to those observed with a 100 mg daily dose in humans (19). In regimen PHZE, rifampin was replaced with high-dose rifapentine (P, 20 mg/kg); this dose in mice approximates the AUC associated with a 1200 mg dose of rifapentine in humans (8, 51). Regimen PHZEC includes both the clofazimine and

rifapentine modifications. Treatment was administered for 12 weeks, and all drugs were administered daily (5 days/week, Monday to Friday) by gavage. Rifampin or rifapentine was administered at least one hour before the HZE combination to avoid adverse pharmacokinetic interactions (52, 53). Clofazimine was administered in a third gavage at least 30 minutes after HZE dosing.

Drug formulations were prepared to deliver the drug and dose in a total volume of 0.2 mL per gavage. For the entire duration of treatment, drug formulations for BALB/c mice were prepared based on an average mouse body mass of 20 g. The body mass of C3HeB/FeJ mice continuously increased over time, and the drug concentrations in each formulation were adjusted accordingly, as detailed in **Table S26**. Rifampin, isoniazid, pyrazinamide, and ethambutol were prepared as solutions in distilled water; clofazimine and rifapentine were prepared as a suspension in 0.05% (wt/vol) agarose. For BALB/c mice, the rifapentine suspension was prepared from crushed tablets; for C3HeB/FeJ mice, the rifapentine suspension was prepared from powder for the first 8 weeks of treatment and from crushed tablets for the last 4 weeks of treatment. Rifapentine tablets (Priftin®) and powder were provided by Sanofi; all other drugs were purchased from Sigma-Aldrich/Millipore Sigma. Drug stocks were prepared weekly in single or multidrug formulations for administration and were stored at 4°C.

Assessment of bactericidal activity

Mice were sacrificed 72 hours after the last dose of treatment was administered. Immediately after euthanasia, blood was collected by cardiac puncture. Lungs were

494 dissected from the mice and stored in 2.5 mL phosphate-buffered saline, pH 7.4, at 4°C
495 for at least 48 hours before gross pathology examination. Lungs were homogenized in
496 TenBroeck glass tissue grinders, and undiluted lung homogenate as well as 10-fold
497 serial dilutions of the homogenate were prepared and cultured as described previously
498 (45), with a volume of 0.5 mL per agar plate. The dilution that yielded CFU counts
499 closest to 50 was used to calculate the total CFU/lung, using the CFU counts from
500 either the plain or charcoal-containing plate, whichever had the higher count, for
501 analysis. Plates were incubated at 37°C in sealed plastic bags for at least 4 weeks
502 before the final reading.
503
504 **Assessment of sterilizing activity**
505 For mice that received PHZEC, PHZE, RHZEC, and RHZE regimens, relapse
506 assessment began after 6, 8, 10, and 12 weeks of treatment, respectively (**Table 1**).
507 These treatment durations were selected based on previous data generated in these
508 mouse models with clofazimine or rifapentine with the first-line regimen (8, 9, 19). Mice
509 were sacrificed 6 months after stopping treatment; lungs were removed, examined, and
510 homogenized as described for the assessment of bactericidal activity. One-tenth of the
511 lung homogenate (0.25 mL) was used to prepare four 10-fold serial dilutions. The entire
512 remaining volume of lung homogenate (2.25 mL) was cultured on four agar plates. To
513 allow approximation of lung CFU counts in the lungs of relapsing mice, the 10^{-2} and 10^{-4}
514 dilutions of lung homogenate were also cultured (0.5 mL per plate). Plates were
515 incubated at 37 °C in sealed plastic bags for at least 6 weeks before the final reading.

Relapse was defined as having culture-positive lungs, *i.e.*, the growth of ≥1 CFU from the lung homogenate.

Media

M. tuberculosis suspensions were grown in 7H9 broth supplemented with a 10% (vol/vol) oleic acid-albumin-dextrose-catalase (OADC) enrichment, 0.5% (vol/vol) glycerol, and 0.1% (vol/vol) Tween 80. Bacterial suspensions (and cognate dilutions) were cultured on 7H11 agar supplemented with 10% (vol/vol) OADC and 0.5% (vol/vol) glycerol (non-selective 7H11 agar). Lung homogenates (and cognate dilutions) were cultured on selective 7H11 agar, *i.e.*, 7H11 agar further supplemented with 50 µg/mL carbenicillin, 10 µg/mL polymyxin B, 20 µg/mL trimethoprim, and 50 µg/mL cycloheximide, to selectively cultivate mycobacteria while inhibiting the growth of contaminating bacteria or fungi (54). To detect and limit drug carryover, lung homogenates from at least all treated mice were plated on selective 7H11 agar further supplemented with an adsorbent agent, 0.4% activated charcoal, as described previously (55). BD Difco Middlebrook 7H9 broth powder, BD Difco Mycobacteria 7H11 agar powder, and BD BBL Middlebrook OADC enrichment were obtained from Becton, Dickinson and Company. Remel Microbiology Products Middlebrook 7H11 agar powder, glycerol, and Tween 80 were obtained from Thermo Fisher Scientific, and activated charcoal was obtained from J. T. Baker. All selective drugs were obtained from Sigma-Aldrich/Millipore Sigma. Stock solutions of trimethoprim were prepared in dimethyl sulfoxide, and all other selective drugs were dissolved in distilled water. Drug stocks were filter sterilized, as was the OADC enrichment, prior to use.

539

540 **Drug concentration determination**

541 Serum was separate from blood samples as previously described (45). Serum samples
542 were stored at -80°C until analysis. Serum clofazimine and rifapentine concentrations
543 were measured by LC-MS/MS and HPLC, respectively, at the Infectious Disease
544 Pharmacokinetics Laboratory at the University of Florida College of Pharmacy,
545 Gainesville, Florida. The lower limits of quantification for clofazimine and rifapentine
546 were 0.01 and 0.5 μg/mL, respectively.

547

548 **Statistical Analyses**

549 All CFU/mL (bacterial suspension) and CFU/lung estimates (x) were log-transformed as
550 $\log_{10}(x + 1)$. For samples cultured in parallel on both plain (*i.e.*, charcoal-free) and
551 charcoal-containing selective 7H11 agar, the $\log_{10}$ CFU/lung determined from the agar
552 type that yielded the higher CFU/lung estimate was used when calculating mean values
553 and standard deviation (SD). The lower limit of detection was calculated based on the
554 proportion of undiluted lung sample cultured. Comparisons of serum drug concentration
555 data and BALB/c lung CFU data between treatment groups and time points were
556 analyzed using two-way analysis of variance corrected with Tukey's test for multiple
557 comparisons. Because of the non-Gaussian distribution of the C3HeB/FeJ lung CFU
558 counts during treatment, comparisons of CFU data between treatment groups and time
559 points were analyzed using the non-parametric Kruskal-Wallis test corrected with
560 Dunn's test for multiple comparisons. The proportions of mice with culture-positive

561 relapse were compared by using Fisher's exact test. All statistical analyses were
562 performed by using GraphPad Prism 7.02.
563
564 **ACKNOWLEDGEMENTS**
565 We thank Jin Lee, Si-Yang Li, Kala Barnes-Boyle, and Jian Xu for help processing the
566 C3HeB/FeJ mice Week 12 relapse samples. Funding for this work was provided by the
567 AIDS Clinical Trials Group, Division of AIDS, National Institutes of Health.
568
569 **REFERENCES**
570 1. World Health Organization. 2018. Global tuberculosis report 2018. WHO reference
571 number: WHO/CDS/TB/2018.20. License: CC BY-NC-SA 3.0 IGO.
572 2. Bloom BR, Atun R. 2016. Back to the future: Rethinking global control of
573 tuberculosis. Sci Transl Med 8:329ps7. doi: 10.1126/scitranslmed.aaf2944.
574 3. World Health Organization. 2017. Guidelines for treatment of drug-susceptible
575 tuberculosis and patient care, 2017 update. WHO/HTM/TB/2017.05. License: CC
576 BY-NC-SA 3.0 IGO.
577 4. Sotgiu G, Nahid P, Loddenkemper R, Abubakar I, Miravitlles M, Migliori GB. 2016.
578 The ERS-endorsed official ATS/CDC/IDSA clinical practice guidelines on treatment
579 of drug-susceptible tuberculosis. Eur Respir J 48:963-971. doi:
580 10.1183/13993003.01356-2016.
581 5. Owens JP, Fofana MO, Dowdy DW. 2013. Cost-effectiveness of novel first-line
582 treatment regimens for tuberculosis. Int J Tuberc Lung Dis 17:590-596. doi:
583 10.5588/ijtld.12.0776.

584 6. Steffen R, Menzies D, Oxlade O, Pinto M, Zuleika de Castro A, Monteiro P, Trajman
585 A. 2010. Patients' costs and cost-effectiveness of tuberculosis treatment in DOTS
586 and non-DOTS facilities in Rio de Janeiro, Brazil. PLoS One 5:e14014. doi:
587 10.1371/journal.pone.0014014.
588 7. Nuermberger EL. 2017. Preclinical Efficacy Testing of New Drug Candidates.
589 Microbiol Spectr 5:2017. doi: 10.1128/microbiolspec.TBTB2-0034-2017.
590 8. Rosenthal IM, Zhang M, Williams KN, Peloquin CA, Tyagi S, Vernon AA, Bishai WR,
591 Chaisson RE, Grosset JH, Nuermberger EL. 2007. Daily dosing of rifapentine cures
592 tuberculosis in three months or less in the murine model. PLoS Med 4:e344. doi:
593 10.1371/journal.pmed.0040344.
594 9. Rosenthal IM, Tasneen R, Peloquin CA, Zhang M, Almeida D, Mdluli KE, Karakousis
595 PC, Grosset JH, Nuermberger EL. 2012. Dose-ranging comparison of rifampin and
596 rifapentine in two pathologically distinct murine models of tuberculosis. Antimicrob
597 Agents Chemother 56:4331-4340. doi: 10.1128/AAC.00912-12.
598 10. Van Deun A, Maug AKJ, Salim MAH, Das PK, Sarker MR, Daru P, Rieder HL. 2010.
599 Short, highly effective, and inexpensive standardized treatment of multidrug-resistant
600 tuberculosis. Am J Respir Crit Care Med 182:684-692. doi: 10.1164/rccm.201001-
601 0077OC.
602 11. Aung KJ, Van Deun A, Declercq E, Sarker MR, Das PK, Hossain MA, Rieder HL.
603 2014. Successful '9-month Bangladesh regimen' for multidrug-resistant tuberculosis
604 among over 500 consecutive patients. Int J Tuberc Lung Dis 18:1180-1187. doi:
605 10.5588/ijtld.14.0100.

606 12. Trébucq A, Schwoebel V, Kashongwe Z, Bakayoko A, Kuaban C, Noeske J,
607 Hassane S, Souleymane B, Piubello A, Ciza F, Fikouma V, Gasana M, Ouedraogo
608 M, Gninafon M, Van Deun A, Cirillo DM, Koura KG, Rieder HL. 2018. Treatment
609 outcome with a short multidrug-resistant tuberculosis regimen in nine African
610 countries. Int J Tuberc Lung Dis 22:17-25. doi: 10.5588/ijtld.17.0498.
611 13. Piubello A, Hassane Harouna S, Souleymane MB, Boukary I, Morou S, Daouda M,
612 Hanki Y, Van Deun A. 2014. High cure rate with standardised short-course
613 multidrug-resistant tuberculosis treatment in Niger: no relapses. Int J Tuberc Lung
614 Dis 18:1188-1194. doi: 10.5588/ijtld.13.0075.
615 14. Tang S, Yao L, Hao X, Liu Y, Zeng L, Liu G, Li M, Li F, Wu M, Zhu Y, Sun H, Gu J,
616 Wang X, Zhang Z. 2015. Clofazimine for the treatment of multidrug-resistant
617 tuberculosis: prospective, multicenter, randomized controlled study in China. Clin
618 Infect Dis 60:1361-1367. doi: 10.1093/cid/civ027.
619 15. Kuaban C, Noeske J, Rieder HL, Aït-Khaled N, Abena Foe JL, Trébucq A. 2015.
620 High effectiveness of a 12-month regimen for MDR-TB patients in Cameroon. Int J
621 Tuberc Lung Dis 19:517-524. doi: 10.5588/ijtld.14.0535.
622 16. Grosset JH, Tyagi S, Almeida DV, Converse PJ, Li SY, Ammerman NC, Bishai WR,
623 Enarson D, Trébucq A. 2013. Assessment of clofazimine activity in a second-line
624 regimen for tuberculosis in mice. Am J Respir Crit Care Med 188:608-612. doi:
625 10.1164/rccm.201304-0753OC.
626 17. World Health Organization. 2016. WHO treatment guidelines for drug-resistant
627 tuberculosis, 2016 update. October 2016 revision. WHO reference number:
628 WHO/HTM/TB/2016.04.

18. Tyagi S, Ammerman NC, Li SY, Adamson J, Converse PJ, Swanson RV, Almeida DV, Grosset JH. 2015. Clofazimine shortens the duration of the first-line treatment regimen for experimental chemotherapy of tuberculosis. Proc Natl Acad Sci U S A 112:869-874. doi: 10.1073/pnas.1416951112.
19. Ammerman NC, Swanson RV, Bautista EM, Almeida DV, Saini V, Omansen TF, Guo H, Chang YS, Li SY, Tapley A, Tasneen R, Tyagi S, Betoudji F, Moodley C, Ngcobo B, Pillay L, Bester LA, Singh SD, Chaisson RE, Nuermberger E, Grosset JH. 2018. Impact of clofazimine dosing on treatment shortening of the first-line regimen in a mouse model of tuberculosis. Antimicrob Agents Chemother 62:636. doi: 10.1128/AAC.00636-18.
20. Grosset J. 2003. *Mycobacterium tuberculosis* in the extracellular compartment: an underestimated adversary. Antimicrob Agents Chemother 47:833-836.
21. Basaraba RJ, Hunter RL. 2017. Pathology of tuberculosis: how the pathology of human tuberculosis informs and directs animal models. Microbiol Spectr 5:2016. doi: 10.1128/microbiolspec.TBTB2-0029-2016.
22. Harper J, Skerry C, Davis SL, Tasneen R, Weir M, Kramnik I, Bishai WR, Pomper MG, Nuermberger EL, Jain SK. 2012. Mouse model of necrotic tuberculosis granulomas develops hypoxic lesions. J Infect Dis 205:595-602. doi: 10.1093/infdis/jir786.
23. Lenaerts A, Barry CE,3rd, Dartois V. 2015. Heterogeneity in tuberculosis pathology, microenvironments and therapeutic responses. Immunol Rev 264:288-307. doi: 10.1111/imr.12252.

651 24. Lanoix JP, Lenaerts AJ, Nuermberger EL. 2015. Heterogeneous disease
652 progression and treatment response in a C3HeB/FeJ mouse model of tuberculosis.
653 Dis Model Mech 8:603-610. doi: 10.1242/dmm.019513.
654 25. Mor N, Simon B, Mezo N, Heifets L. 1995. Comparison of activities of rifapentine
655 and rifampin against *Mycobacterium tuberculosis* residing in human macrophages.
656 Antimicrob Agents Chemother 39:2073-2077. doi: 10.1128/AAC.39.9.2073.
657 26. Baik J, Rosania GR. 2012. Macrophages sequester clofazimine in an intracellular
658 liquid crystal-like supramolecular organization. PLoS One 7:e47494. doi:
659 10.1371/journal.pone.0047494.
660 27. Prideaux B, Via LE, Zimmerman MD, Eum S, Sarathy J, O'Brien P, Chen C, Kaya F,
661 Weiner DM, Chen PY, Song T, Lee M, Shim TS, Cho JS, Kim W, Cho SN, Olivier
662 KN, Barry CE,3rd, Dartois V. 2015. The association between sterilizing activity and
663 drug distribution into tuberculosis lesions. Nat Med 21:1223-1227. doi:
664 10.1038/nm.3937.
665 28. Rifat D, Prideaux B, Savic RM, Urbanowski ME, Parsons TL, Luna B, Marzinke MA,
666 Ordonez AA, DeMarco VP, Jain SK, Dartois V, Bishai WR, Dooley KE. 2018.
667 Pharmacokinetics of rifapentine and rifampin in a rabbit model of tuberculosis and
668 correlation with clinical trial data. Sci Transl Med 10:eaai7786. doi:
669 10.1126/scitranslmed.aai7786.
670 29. Savic RM, Weiner M, MacKenzie WR, Engle M, Whitworth WC, Johnson JL,
671 Nsubuga P, Nahid P, Nguyen NV, Peloquin CA, Dooley KE, Dorman SE,
672 Tuberculosis Trials Consortium of the Centers for Disease Control and Prevention.
673 2017. Defining the optimal dose of rifapentine for pulmonary tuberculosis: exposure-

response relations from two phase II clinical trials. Clin Pharmacol Ther 102:321-331. doi: 10.1002/cpt.634.

30. Irwin SM, Gruppo V, Brooks E, Gilliland J, Scherman M, Reichlen MJ, Leistikow R, Kramnik I, Nuermberger EL, Voskuil MI, Lenaerts AJ. 2014. Limited activity of clofazimine as a single drug in a mouse model of tuberculosis exhibiting caseous necrotic granulomas. Antimicrob Agents Chemother 58:4026-4034. doi: 10.1128/AAC.02565-14.

31. Pan H, Yan BS, Rojas M, Shebzukhov YV, Zhou H, Kobzik L, Higgins DE, Daly MJ, Bloom BR, Kramnik I. 2005. *Ipr1* gene mediates innate immunity to tuberculosis. Nature 434:767-772. doi: 10.1038/nature03419.

32. Ordonez AA, Tasneen R, Pokkali S, Xu Z, Converse PJ, Klunk MH, Mollura DJ, Nuermberger EL, Jain SK. 2016. Mouse model of pulmonary cavitary tuberculosis and expression of matrix metalloproteinase-9. Dis Model Mech 9:779-788. doi: 10.1242/dmm.025643.

33. Davis SL, Nuermberger EL, Um PK, Vidal C, Jedynak B, Pomper MG, Bishai WR, Jain SK. 2009. Noninvasive pulmonary [^{18}F]-2-fluoro-deoxy-D-glucose positron emission tomography correlates with bactericidal activity of tuberculosis drug treatment. Antimicrob Agents Chemother 53:4879-4884. doi: 10.1128/AAC.00789-09.

34. Driver ER, Ryan GJ, Hoff DR, Irwin SM, Basaraba RJ, Kramnik I, Lenaerts AJ. 2012. Evaluation of a mouse model of necrotic granuloma formation using C3HeB/FeJ mice for testing of drugs against *Mycobacterium tuberculosis*. Antimicrob Agents Chemother 56:3181-3195. doi: 10.1128/AAC.00217-12.

697 35. Irwin SM, Driver E, Lyon E, Schrupp C, Ryan G, Gonzalez-Juarrero M, Basaraba
698 RJ, Nuermberger EL, Lenaerts AJ. 2015. Presence of multiple lesion types with
699 vastly different microenvironments in C3HeB/FeJ mice following aerosol infection
700 with *Mycobacterium tuberculosis*. Dis Model Mech 8:591-602. doi:
701 10.1242/dmm.019570.
702 36. Li SY, Irwin SM, Converse PJ, Mdluli KE, Lenaerts AJ, Nuermberger EL. 2015.
703 Evaluation of moxifloxacin-containing regimens in pathologically distinct murine
704 tuberculosis models. Antimicrob Agents Chemother 59:4026-4030. doi:
705 10.1128/AAC.00105-15.
706 37. Lanoix JP, Betoudji F, Nuermberger E. 2015. Sterilizing activity of pyrazinamide in
707 combination with first-line drugs in a C3HeB/FeJ mouse model of tuberculosis.
708 Antimicrob Agents Chemother 60:1091-1096. doi: 10.1128/AAC.02637-15.
709 38. Ordonez AA, Pokkali S, Kim S, Carr B, Klunk MH, Tong L, Saini V, Chang YS,
710 McKevitt M, Smith V, Gossage DL, Jain SK. 2018. Adjunct antibody administration
711 with standard treatment reduces relapse rates in a murine tuberculosis model of
712 necrotic granulomas. PLoS One 13:e0197474. doi: 10.1371/journal.pone.0197474.
713 39. Driver, E. R. 2014. The C3HeB/FeJ mice as a novel preclinical mouse model for
714 *Mycobacterium tuberculosis*: an analysis of the host pathogenesis and the *in vivo*
715 environment of the necrotic granuloma. Doctor of Philosophy (Ph.D.). Colorado
716 State University, Fort Collins, Colorado.
717 40. Rosenthal IM, Zhang M, Almeida D, Grosset JH, Nuermberger EL. 2008. Isoniazid
718 or moxifloxacin in rifapentine-based regimens for experimental tuberculosis? Am J
719 Respir Crit Care Med 178:989-993. doi: 10.1164/rccm.200807-1029OC.

720 41. Sarathy JP, Via LE, Weiner D, Blanc L, Boshoff H, Eugenin EA, Barry CE,3rd,
721 Dartois VA. 2018. Extreme drug tolerance of *Mycobacterium tuberculosis* in caseum.
722 Antimicrob Agents Chemother 62:2266. doi: 10.1128/AAC.02266-17.
723 42. Conalty ML, Jackson RD. 1962. Uptake by reticulo-endothelial cells of the
724 riminophenazine B.663 (2-*p*-chloroanilino-5-*p*-chlorophenyl-3 : 5-dihydro-3-
725 isopropyliminophenazine). Br J Exp Pathol 43:651-654.
726 43. Schump MD, Fox DM, Bertozzi CR, Riley LW. 2017. Subcellular partitioning and
727 intramacrophage selectivity of antimicrobial compounds against *Mycobacterium*
728 *tuberculosis*. Antimicrob Agents Chemother 61:1639. doi: 10.1128/AAC.01639.
729 44. Dorman SE, Goldberg S, Stout JE, Muzanyi G, Johnson JL, Weiner M, Bozeman L,
730 Heilig CM, Feng PJ, Moro R, Narita M, Nahid P, Ray S, Bates E, Haile B,
731 Nuermberger EL, Vernon A, Schluger NW, Tuberculosis Trials Consortium. 2012.
732 Substitution of rifapentine for rifampin during intensive phase treatment of pulmonary
733 tuberculosis: study 29 of the tuberculosis trials consortium. J Infect Dis 206:1030-
734 1040. doi: 10.1093/infdis/jis461.
735 45. Ammerman NC, Swanson RV, Tapley A, Moodley C, Ngcobo B, Adamson J,
736 Dorasamy A, Moodley S, Mgaga Z, Bester LA, Singh SD, Almeida DV, Grosset JH.
737 2017. Clofazimine has delayed antimicrobial activity against *Mycobacterium*
738 *tuberculosis* both *in vitro* and *in vivo*. J Antimicrob Chemother 72:455-461. doi:
739 10.1093/jac/dkw417.
740 46. Swanson RV, Ammerman NC, Ngcobo B, Adamson J, Moodley C, Dorasamy A,
741 Moodley S, Mgaga Z, Bester LA, Singh SD, Almeida DV, Grosset JH. 2016.
742 Clofazimine contributes sustained antimicrobial activity after treatment cessation in a

743 mouse model of tuberculosis chemotherapy. Antimicrob Agents Chemother 60:2864-
744 2869. doi: 10.1128/AAC.00177-16.
745 47. Swanson RV, Adamson J, Moodley C, Ngcobo B, Ammerman NC, Dorasamy A,
746 Moodley S, Mgaga Z, Tapley A, Bester LA, Singh S, Grosset JH, Almeida DV. 2015.
747 Pharmacokinetics and pharmacodynamics of clofazimine in the mouse model of
748 tuberculosis. Antimicrob Agents Chemother 59:3042-3051. doi: 10.1129/AAC.00260-
749 15.
750 48. Tucker EW, Guglieri-Lopez B, Ordonex AA, Ritchie B, Klunk MH, Sharma R, Chang
751 YS, Sanchez-Bautista J, Frey S, Lodge MA, Rowe SP, Hold DP, Gobburu J,
752 Peloquin CA, Mathews WB, Dannals RF, Pardo CA, Kannan S, Ivaturi V, Jain SK.
753 2018. Noninvasive ^{11}C-rifampin positron emission tomography reveals drug
754 biodistribution in tuberculous meningitis. Sci Transl Med 10: eaau0965. doi:
755 10.1126/scitranslmed.aau0965.
756 49. Almeida D, Nuermberger E, Tasneen R, Rosenthal I, Tyagi S, Williams K, Peloquin
757 C, Grosset J. 2009. Paradoxical effect of isoniazid on the activity of rifampin-
758 pyrazinamide combination in a mouse model of tuberculosis. Antimicrob Agents
759 Chemother 53:4178-4184. doi: 10.1128/AAC.00830-09.
760 50. Grosset J, Ji B. 1998. Experimental chemotherapy of mycobacterial diseases, p. 51-
761 97. *In* P. R. J. Gangadharam and P. A. Jenkins (eds.), Mycobacteria Volume II
762 Chemotherapy. Chapman & Hall, New York.
763 51. Rosenthal IM, Williams K, Tyagi S, Vernon AA, Peloquin CA, Bishai WR, Grosset
764 JH, Nuermberger EL. 2005. Weekly moxifloxacin and rifapentine is more active than

765 the Denver regimen in murine tuberculosis. Am J Respir Crit Care Med 172:1457-
766 1462. doi: 10.1164/rccm.200507-1072OC.
767 52. Grosset J, Truffot-Pernot C, Lacroix C, Ji B. 1992. Antagonism between isoniazid
768 and the combination pyrazinamide-rifampin against tuberculosis infection in mice.
769 Antimicrob Agents Chemother 36:548-551. doi: 10.1128/AAC.36.3.548.
770 53. Dhillon J, Dickinson JM, Sole K, Mitchison DA. 1996. Preventive chemotherapy of
771 tuberculosis in Cornell model mice with combinations of rifampin, isoniazid, and
772 pyrazinamide. Antimicrob Agents Chemother 40:552-555. doi:
773 10.1128/AAC.40.3.552.
774 54. Mitchison DA, Allen BW, Carrol L, Dickinson JM, Aber VR. 1972. A selective oleic
775 acid albumin agar medium for tubercle bacilli. J Med Microbiol 5:165-175. doi:
776 10.1099/00222615-5-2-165.
777 55. Tasneen R, Li SY, Peloquin CA, Taylor D, Williams KN, Andries K, Mdluli KE,
778 Nuermberger EL. 2011. Sterilizing activity of novel TMC207- and PA-824-containing
779 regimens in a murine model of tuberculosis. Antimicrob Agents Chemother 55:5485-
780 5492. doi: 10.1128/AAC.05293-11.

781 **FIGURES**

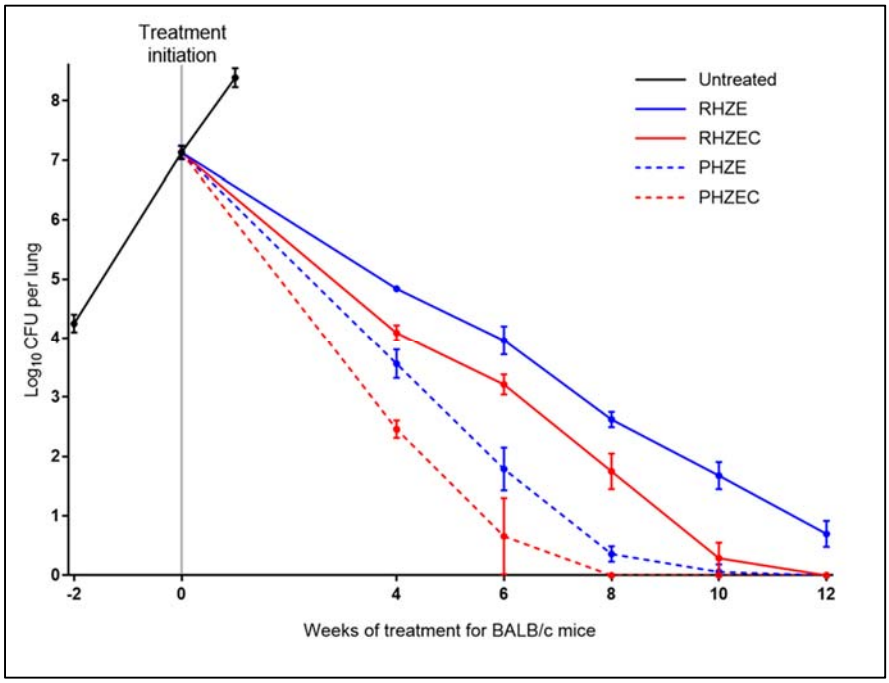

782

783 **Figure 1. Lung CFU counts of BALB/c mice before and during treatment.** Data
784 points represent mean values, and error bars represent the SD (3-9 mice per group per
785 time point). Treatment regimens are described in **Table 1**. Raw CFU data are presented
786 in **Table S2** (Week -2/day after infection), **Table S3** (Day 0 and Untreated group), and
787 **Tables S4**, **S5**, **S6**, **S7**, and **S8** (Week 4, 6, 8, 10, and 12, respectively).

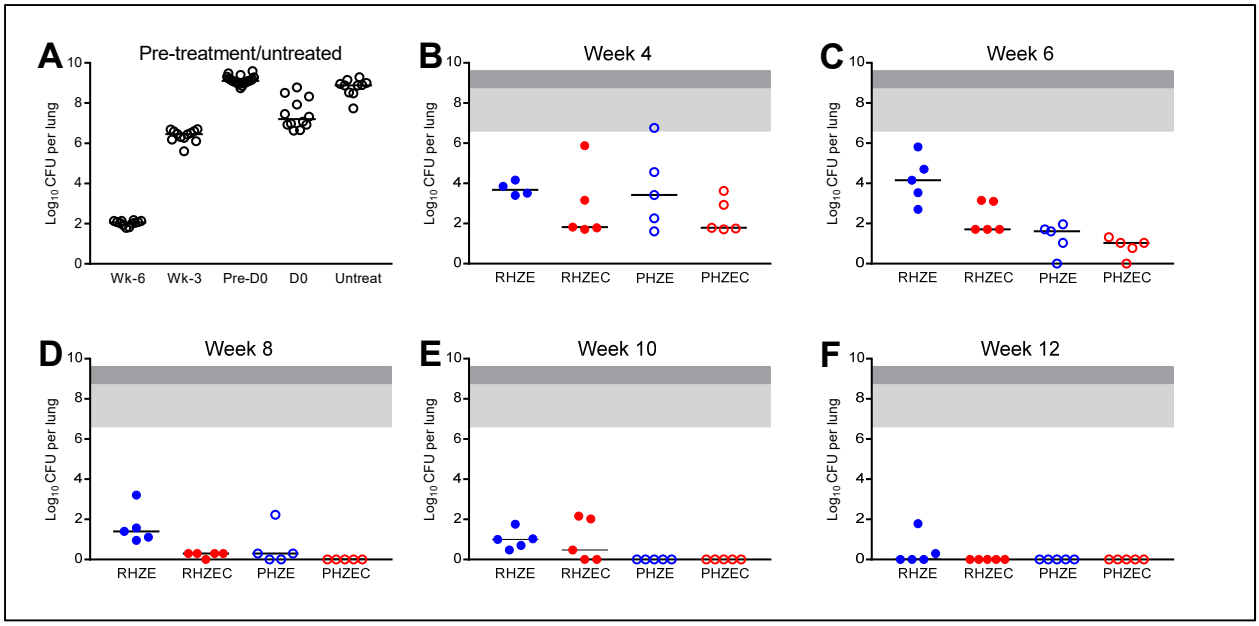

Figure 2. Lung CFU counts of C3HeB/FeJ mice before and during treatment. Lung CFU counts from mice sacrificed the day after infection ("Wk-6"), three weeks after infection ("Wk-3"), and on the day of treatment initiation ("D0") are shown in **Panel A**, as are the lung CFU counts are for mice that became moribund and were euthanized after Wk-3 but before D0 ("Pre-D0") and for the untreated negative control mice ("Untreat"). Lung CFU counts after 4, 6, 8, 10, and 12 weeks of treatment are shown in **Panels B**, **C**, **D**, **E**, and **F**, respectively. Treatment regimens are described in **Table 1**. Due to the variability associated with this model, the lung CFU counts were plotted by individual mouse, with the median value indicated with a black bar. For panels B-F, the area shaded light gray indicates the range of lung CFU counts at the start of treatment in the mice sacrificed at D0, and the area shaded dark gray extends the range to include the lung CFU counts of the mice that died prior to D0. Raw CFU data are presented in **Table S2** (Wk-6), **Table S13** (Wk-3, D0), **Table S14** (Pre-D0, Untreated), and **Tables S15**, **S16**, **S17**, **S18**, and **S19** (Week 4, 6, 8, 10, and 12, respectively).

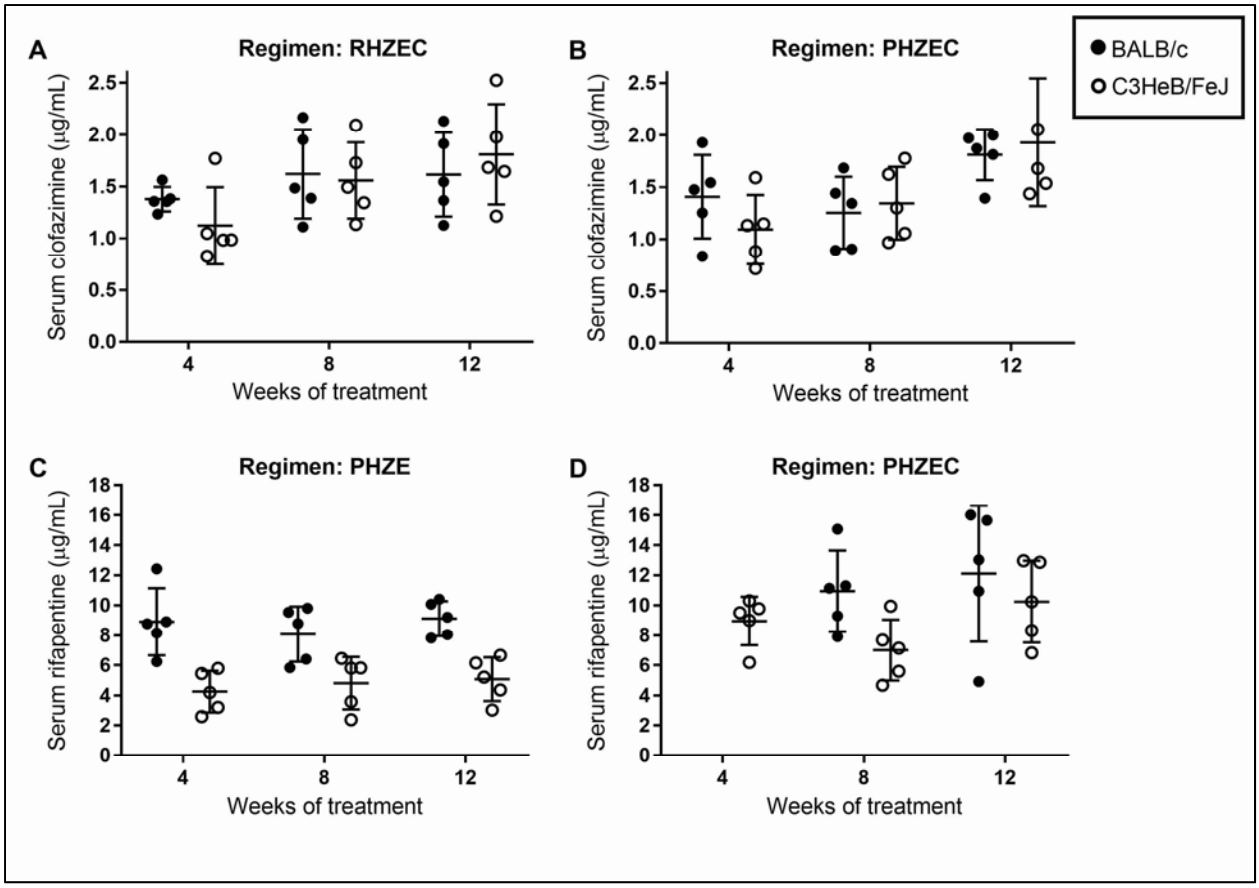

Figure 3. Trough serum clofazimine (Panels A,B) and rifapentine (Panels C,D) concentrations during treatment in BALB/c and C3HeB/FeJ. Serum samples were obtained at sacrifice (about 72 hours after dosing) from mice treated for 4, 8, and 12 weeks. Serum clofazimine levels were determined in mice treated with RHZEC **(Panel A)** and PHZEC (**Panel B**). Serum rifapentine levels were determined in mice treated with PHZE (**Panel C**) and PHZEC (**Panel D**). Individual data points (5 mice per group per time point) are plotted as well as mean and standard deviation values (error bars). For BALB/c mice, the PHZEC Week 4 samples for rifapentine measurement were compromised and discarded. Concentration data for each mouse are presented in **Table S24**.

814 # TABLES

815 ## Table 1. Final experiment scheme for BALB/c and C3HeB/FeJ mouse models.

816

Mouse strain and regimen[a]	Number of mice[b] withdrawn from treatment for sacrifice (CFUs) or relapse assessment[c] at the following time points:													Total mice
	Week -6	Week -3	Week -2	Day 0	Week 4	Week 6		Week 8		Week 10		Week 12		
	CFUs	CFUs	CFUs	CFUs	CFUs	CFUs	Relapse	CFUs	Relapse	CFUs	Relapse	CFUs	Relapse	
BALB/c mice														
Untreated[d]			9	9	9									27
RHZE					5	5		5		5		5	20	45
RHZEC					5	5		5		5	18	5	20	63
PHZE					5	5		5	18	5	18	5	20	81
PHZEC					5	5	18	5	18	5	18	5	20	99
Total BALB/c mice			9	9	29	20	18	20	36	20	54	20	80	315
C3HeB/FeJ mice														
Untreated[d,e]	12	12	17	12	12									65
RHZE					5	5		5		5		5	20	45
RHZEC					5	5		5		5	18	5	20	63
PHZE					5	5		5	18	5	18	5	20	81
PHZEC					5	5	18	5	18	5	18	5	20	99
Total C3HeB/FeJ mice	12	12	17	12	32	20	18	20	36	20	54	20	80	353

[a] Treatment was initiated on Day 0. Regimens were comprised of the following drugs and doses: R, rifampin 10 mg/kg; H, isoniazid 10 mg/kg; Z, pyrazinamide 150 mg/kg; E, ethambutol 100 mg/kg; C, clofazimine 12.5 mg/kg; P, rifapentine 20 mg/kg.

[b] Any discrepancies in the number of mice presented in this table and the number of mice from which data were obtained are accounted for in the supplemental raw CFU data tables associated with each mouse strain and time point.

[c] Relapse was assessed 6 months after stopping treatment.

[d] Untreated negative control mice (three from each infection run) were followed after Day 0 to verify *M. tuberculosis* virulence. Although included under the Week 4 time point for simplicity, these mice were euthanized at varying time points when they became moribund.

[e] Seventeen mice were moribund and euthanized after Week -3 but before Day 0; for simplicity, they are included in this table under the Week -2 time point.

817

818 **Table 2. Relapse results determined 6 months after stopping treatment.**

Regimen[a]	Mouse strain	Proportion of mice with culture-positive relapse by treatment duration			
		6 weeks	8 weeks	10 weeks	12 weeks
RHZE	BALB/c	---	---	---	19/20
	C3HeB/FeJ	---	---	---	11/19
RHZEC	BALB/c	---	---	10/18	0/20
	C3HeB/FeJ	---	---	7/17	3/18
PHZE	BALB/c	---	6/20	1/18	0/18
	C3HeB/FeJ	---	10/18	0/17	2/20
PHZEC	BALB/c	5/18	0/18	2/18	0/20
	C3HeB/FeJ	5/17	1/18	1/18	0/18

[a]Regimens are described in **Table 1**.

--- indicates not determined.

819